Journal of Nanotechnology and Innovative Materials

Research Article

Effect of Tunnelling on the Thermoelectric Efficiency of Bulk Nanostructured $Bi_{0.5}Sb_{1.5}Te_3$ Materials

Sayyara A. Nabieva[1], Durdana F. Rustamova[2], Ogtay B. Taghiyev[1], Vafa Hajiyeva[1], and Gulnara Huseynova[1]

[1]Institute of Physics, Ministry of Science and Education, 131 H. Javid Avenue, AZ1143 Baku, Azerbaijan
[2]Department of Mechanics and Mathematics, School of Advanced Technologies and Innovation Engineering, Western Caspian University, Ahmad Rajabli 17A, III Parallel, AZ1001 Baku, Azerbaijan

Received: 28.02.2026 Accepted: 20.07.2026 Published: 31.07.2026

https://doi.org/10.54414/QVBK6661

Abstract

This work investigates the influence of electron tunnelling on the kinetic and thermoelectric properties of nanostructured bulk materials based on $Bi_{0.5}Sb_{1.5}Te_3$. The study focuses on systems where electric transport occurs through a network of semiconducting grains separated by narrow dielectric barriers of nanometer-scale thickness. In this regime, the dominant conduction mechanism is tunnelling, and phonon heat transfer across the barriers can be neglected. Numerical evaluation of the electrical conductivity, thermal conductivity, Seebeck coefficient, and the effective thermoelectric figure of merit (ZT) demonstrates that tunnelling can significantly enhance the thermoelectric voltage and lead to $ZT \approx 1–2$ at room temperature, even though the overall electrical conductivity remains relatively low. These results suggest that properly engineered tunnelling contacts can serve as an efficient mechanism for improving energy conversion in bulk thermoelectric composites.

Keywords: thermoelectric materials, $Bi_{0.5}Sb_{1.5}Te_3$, electron tunnelling, nanostructured composites, Seebeck coefficient, thermal conductivity

1. Introduction

Thermoelectric materials based on Bi–Sb–Te compounds remain among the most efficient systems for room-temperature energy conversion [1], [2], [3]. In recent years, nanostructuring has emerged as a way to enhance thermoelectric performance by suppressing phonon transport, modifying carrier scattering, and altering the electronic density of states [1], [3], [4]. One promising route involves constructing bulk nanocomposites in which semiconductor grains are embedded within a dielectric matrix, forming a network of nanoscale tunnelling junctions [5], [6], [7]. Our system works like this: a network of semiconducting grains, each separated from its neighbours by very narrow dielectric barriers only nanometres thick [8], [9], [10].

The overall transport properties of such a system are governed by both the internal conductivity of the grains and the transmission probability of the tunnelling barriers [5], [6], [11]. For typical Bi–Sb–Te systems, the barrier height is close to 0.8 eV [2], [11].

When the characteristic dimensions of the tunnelling region are shorter than the electron mean free path, carriers pass through the barrier ballistically, eliminating ohmic losses typically associated with scattering [5], [11], [12]. This quantum-mechanical contribution significantly modifies the effective transport coefficients of the composite material and may enhance its energy conversion efficiency.

2. Theoretical Model and Calculation Method

The thermoelectric efficiency of nanostructured $Bi_{0.5}Sb_{1.5}Te_3$ composites was investigated assuming that nanometre-scale dielectric barriers separate semiconductor grains. In such systems, charge transport occurs through tunnelling contacts formed between adjacent grains [5], [6], [11].

The transport mechanism through the tunnelling barrier is assumed to be ballistic, meaning that the barrier thickness is smaller than the electron free path. Under these conditions, electrons pass through the barrier without scattering, and the transmission probability strongly depends on the barrier thickness and height [5], [11].

The equation for the local electrical conductivity (1.1) is expressed as:

$$\sigma_M(x) = \frac{x+\delta}{\frac{x}{\sigma_b(x)} + \frac{\delta}{\sigma} + \frac{(\alpha_b(x)-\alpha)^2}{\delta \cdot \kappa_b(x) + x\kappa}\,\delta x T} \qquad (1.1)$$

Here:

σ_M (x) – local electrical conductivity;
x – tunneling barrier thickness;
δ – characteristic grain size;
σ_b (x) – electrical conductivity of the tunneling barrier;
σ – electrical conductivity of the semiconductor grain;
α_b (x) – barrier Seebeck coefficient;
α – grain Seebeck coefficient;
κ_b (x) – barrier thermal conductivity;
κ - grain thermal conductivity.

The equation for local thermal conductivity (1.2) is determined by:

$$\kappa_M(x) = \frac{x+\delta}{\frac{x}{\kappa_b(x)} + \frac{\delta}{\kappa}} \qquad (1.2)$$

The equation for the local Seebeck coefficient (1.3) is calculated as:

$$\alpha_M(x) = \frac{\frac{\alpha_b(x)}{\kappa_b(x)}x + \frac{\alpha}{\kappa}\delta}{\frac{x}{\kappa_b(x)} + \frac{\delta}{\kappa}} \qquad (1.3)$$

The effective electrical conductivity and thermal conductivity are determined numerically from the integral equations.

The effective electrical conductivity equation (1.4) is expressed as:

$$\int_{x_{min}}^{x_{\max}} \frac{\sigma_e - \sigma_M(x)}{2\sigma_e + \sigma_M(x)} D(x)dx = 0 \qquad (1.4)$$

D (x) – distribution function of barrier thicknesses.

The effective thermal conductivity equation (1.5) is determined by:

$$\int_{x_{\min}}^{x_{\max}} \frac{\kappa_e - \kappa_M(x)}{2\kappa_e + \kappa_M(x)} D(x)dx = 0 \quad (1.5)$$

The effective Seebeck coefficient equation (1.6) is calculated as:

$$\alpha_e = \frac{\int_{x_{\min}}^{x_{\max}} \frac{\alpha_M(x)\sigma_M(x)}{\Delta_0(x)} D(x)dx}{\int_{x_{\min}}^{x_{\max}} \frac{\sigma_M(x)}{\Delta_0(x)} D(x)dx} \quad (1.6)$$

After determining the effective electrical conductivity σ_e, thermal conductivity κ_e, and Seebeck coefficient α_e, the thermoelectric figure of merit was calculated using (1.7):

$$ZT = \frac{\sigma\alpha^2 T}{\kappa} \quad (1.7)$$

σ_e – effective electrical conductivity;
α_e – effective Seebeck coefficient;
κ_e – effective thermal conductivity;
T – absolute temperature.

For numerical calculations, the tunnelling barrier height for $Bi_{0.5}Sb_{1.5}Te_3$ was assumed to be 0.8 eV. The calculations were performed at T = 300 K using Mathematica software. The experimentally determined transport parameters for bulk $Bi_{0.5}Sb_{1.5}Te_3$ used in the model were:

$\sigma = 7.0 \times 10^4\ \Omega^{-1}\ m^{-1}$
k = 1.02 W/(m·K)
$\alpha = 200\ \mu V/K$

The thermal conductivity of the tunnelling barrier was estimated using the Lorenz/Wiedemann–Franz relation (1.8) [13].

$$\kappa_b = TL_b\sigma_b \quad (1.8)$$

L – Lorenz number;
σ_b – barrier conductivity;
T – temperature.

The local electrical conductivity $\sigma_a(x)$ (1.9) is given by:

$$\sigma_a(x) = (x + \delta) / [x/\sigma_b(x) + \delta/\sigma + ((\alpha_b(x) - \alpha)^2 / (\delta\cdot\kappa_b(x) + x\cdot\kappa)) \cdot \delta\cdot x\cdot T] \quad (1.9)$$

x – tunnelling barrier thickness;
δ – characteristic grain size;
$\sigma_b(x)$ – conductivity of the barrier;
σ – conductivity of the grain;
$\alpha_b(x)$ – Seebeck coefficient of the barrier;

α – Seebeck coefficient of the grain;
$\kappa\_b(x)$ – thermal conductivity of the barrier;
κ – thermal conductivity of the grain.

The local thermal conductivity $\kappa_a(x)$ (1.10) is:

$$\kappa_a(x) = (x + \delta) / (x/\kappa\_b(x) + \delta/\kappa) \qquad (1.10)$$

The local Seebeck coefficient $\alpha_a(x)$ (1.11) is:

$$\alpha_a(x) = [(\alpha\_b(x)/\kappa\_b(x))\ x + (\alpha/\kappa)\cdot\delta] / [x/\kappa\_b(x) + \delta/\kappa] \qquad (1.11)$$

To get the effective electrical and thermal conductivities of the whole composite, we solved these integral equations (1.12), (1.13):

$$\int [(\sigma_e - \sigma_a(x)) / (2\sigma_e + \sigma_a(x))] \cdot D(x)\ dx = 0 \qquad (1.12)$$

$$\int [(\kappa_e - \kappa_a(x)) / (2\kappa_e + \kappa_a(x))] \cdot D(x)\ dx = 0 \qquad (1.13)$$

$D(x)$ – distribution of barrier thicknesses.

The effective Seebeck coefficient (1.14), (1.15) came from:

$$\alpha_e = \int [(\alpha_a(x)\cdot\sigma_a(x)) / \Delta_0(x)] \cdot D(x)\ dx \ / \ \int [\sigma_a(x) / \Delta_0(x)] \cdot D(x)\ dx \qquad (1.14)$$

$$\text{with} \quad \Delta_0(x) = (2\sigma_e + \sigma_a(x)) \cdot (2\kappa_e + \kappa_a(x)) \qquad (1.15)$$

Once we had σ_e, κ_e, and α_e, we calculated the figure of merit (1.16):

$$ZT = (\sigma_e \cdot \alpha_e^2 \cdot T) / \kappa_e \qquad (1.16)$$

3. Results and Discussion

Figure 1 shows the dependence of the effective electrical conductivity on the minimum thickness of the tunnelling barrier.

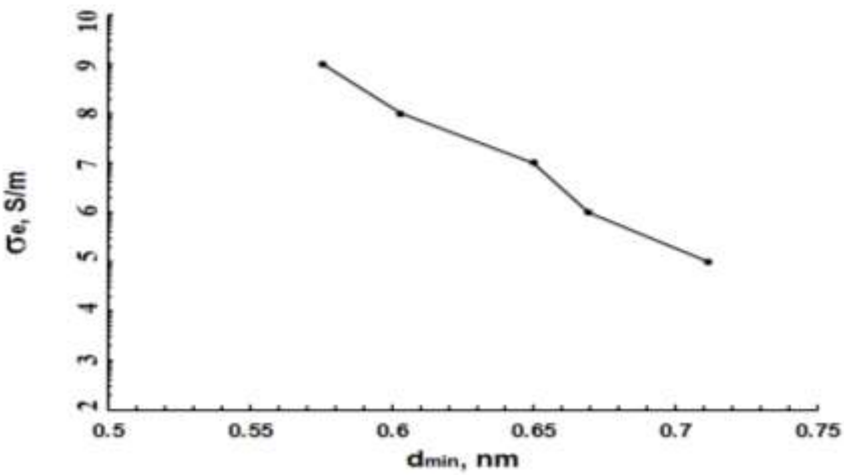

Figure 1. Dependence of the effective electrical conductivity on the minimum tunnelling barrier thickness [6].

The conductivity decreases exponentially as the barrier thickness increases. This behaviour is characteristic of quantum tunnelling transport because the tunnelling probability rapidly decreases with increasing barrier width [5], [6], [11]. For ultrathin barriers, electrons can pass through the contact with relatively low resistance, whereas thicker barriers strongly suppress carrier transport.

Figure 2 presents the calculated dependence of thermal conductivity on the tunnelling barrier thickness. Similar to electrical conductivity, the thermal conductivity also decreases with increasing barrier thickness. However, the reduction in thermal conductivity is especially important for improving thermoelectric efficiency because phonon transport is suppressed more strongly than electronic transport in the tunnelling region [1], [3], [7].

The comparatively low thermal conductivity of the tunnelling barrier contributes to the enhancement of thermoelectric performance by reducing heat leakage through the composite structure.

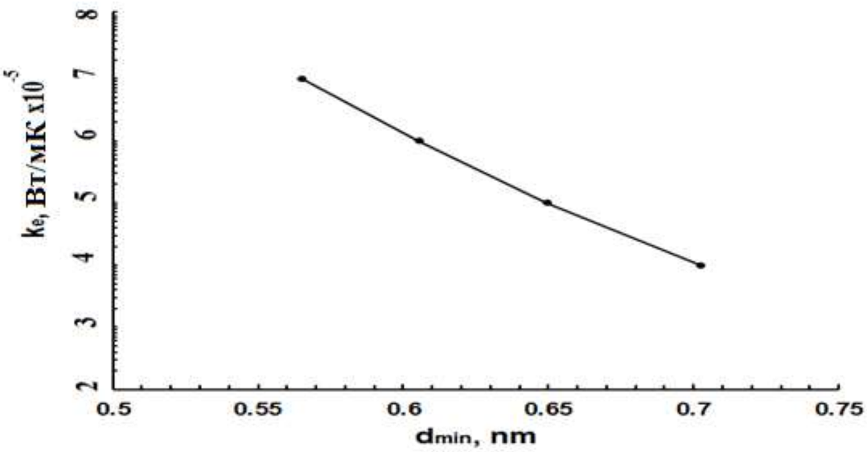

Figure 2. Calculated dependence of thermal conductivity on the minimum tunnelling barrier thickness [6].

Figure 3 illustrates the dependence of the effective Seebeck coefficient on the minimum tunnelling barrier thickness. The Seebeck coefficient increases as the barrier thickness decreases. This effect can be explained by the energy filtering of charge carriers inside the tunnelling barrier [3], [4]. Electrons with higher energy have a greater probability of transmission through the barrier, which increases the average carrier energy and therefore enhances the thermoelectric voltage.

The energy filtering effect observed in the model is consistent with previously reported tunnelling and low-dimensional thermoelectric systems [3], [4], [12], [14], [15].

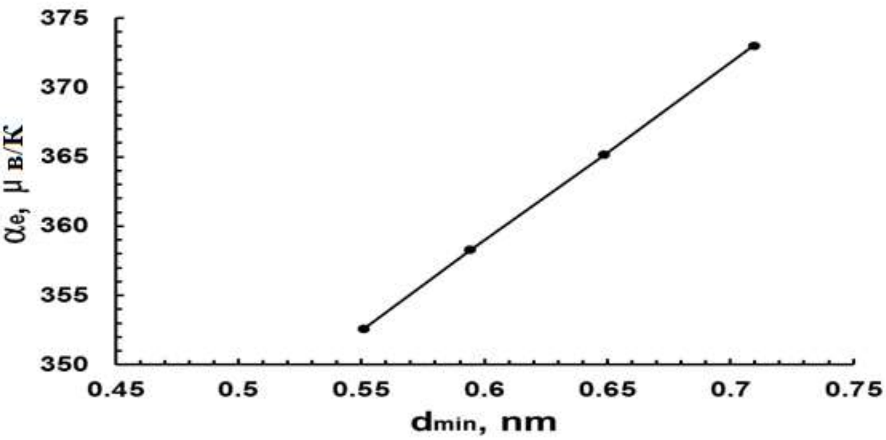

Figure 3. Dependence of the effective Seebeck coefficient on the minimum tunnelling barrier thickness [6].

Figure 4 shows the calculated dependence of the thermoelectric figure of merit *ZT* on the tunnelling barrier thickness. The results indicate that *ZT* increases significantly for ultrathin tunnelling barriers. According to the theoretical model, the effective thermoelectric efficiency may approach values close to $ZT \approx 1–2$ under idealized tunnelling conditions at room temperature.

The enhancement of thermoelectric efficiency is primarily associated with the strong suppression of thermal conductivity, together with the simultaneous increase in the Seebeck coefficient. Although the electrical conductivity decreases with increasing barrier thickness, the reduction in heat transport dominates, leading to an overall increase in *ZT*.

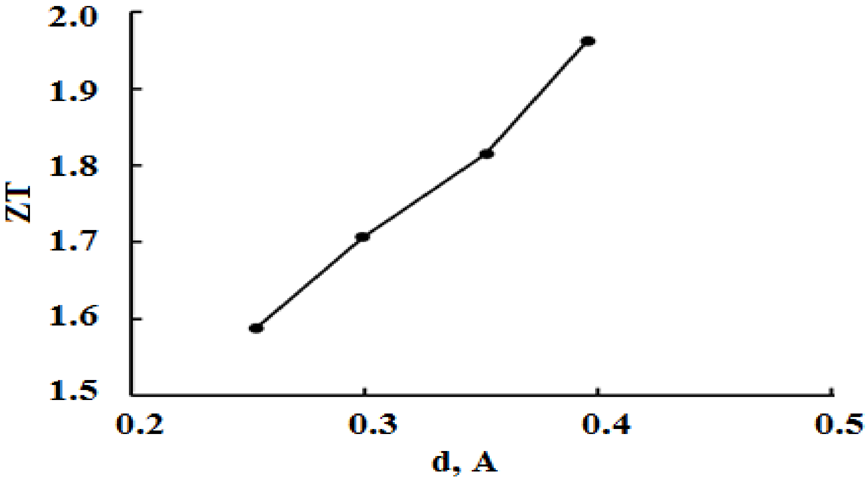

Figure 4. Calculated dependence of the thermoelectric figure of merit *ZT* on the minimum tunnelling barrier thickness [6].

The obtained results demonstrate that the thermoelectric properties of nanostructured $Bi_{0.5}Sb_{1.5}Te_3$ composites are highly sensitive to the geometric parameters of the tunnelling contacts, particularly the barrier thickness. Therefore, precise control of nanoscale barrier formation may provide an effective route for improving thermoelectric energy conversion efficiency.

4. Conclusion

This work demonstrates that tunnelling transport in nanostructured $Bi_{0.5}Sb_{1.5}Te_3$ composites can significantly modify their thermoelectric properties. The presence of nanometre-scale barriers leads to a substantial reduction of thermal conductivity while preserving or enhancing the Seebeck coefficient. As a result, the effective thermoelectric efficiency can reach values of $ZT \approx 1–2$ at room temperature. The influence of barrier geometry, grain shape, and material distribution is secondary compared to the dominant role of barrier thickness and height. These results confirm that engineering tunnelling junctions is a promising approach for designing next-generation high-efficiency thermoelectric materials. The behaviour predicted by the model is qualitatively consistent with experimental reports on nanostructured Bi_2Te_3-based materials, in which enhancements in ZT have been observed due to grain-boundary scattering and energy filtering [1], [3], [4]. However, the current model uniquely demonstrates that quantum tunnelling alone, without the involvement of phonon engineering techniques, is sufficient to produce $ZT \approx 1–2$, a significant theoretical insight. Furthermore, the results agree with the predictions of Dresselhaus (2007) regarding the benefits of nanoscale confinement but provide a different physical mechanism applicable to bulk composites [3].

Author Contributions

All authors reviewed, edited, and approved the manuscript.

Conflict of Interest

The authors declare no conflicts of interest.

Funding

This research received no external funding.

Acknowledgment

The authors declare no acknowledgments.

Abbreviations

Thermoelectric Figure of Merit (ZT), Bismuth–Antimony Telluride ($Bi_{0.5}Sb_{1.5}Te_3$).

References

[1] Bulat LP, Osvenskii VB, Parkhomenko YN, Pshenai-Severin DA. Investigation of the possibilities for increasing the thermoelectric figure of merit of nanostructured materials based on Bi2Te3-Sb2Te3 solid solutions. Physics of the Solid State. 2012 Nov;54(11):2165-72. https://doi.org/10.1134/s1063783412110054
[2] Goltsman BM, Kudinov VA, Smirnov IA. Semiconductor thermoelectric materials based on Bi2Te3.
[3] Dresselhaus MS, Chen G, Tang MY, Yang RG, Lee H, Wang DZ, Ren ZF, Fleurial JP, Gogna P. New directions for low-dimensional thermoelectric materials. Advanced Materials. 2007 Apr 20;19(8):1043-53. https://doi.org/10.1002/adma.200600527
[4] Harman TC, Taylor PJ, Walsh MP, LaForge BE. Quantum dot superlattice thermoelectric materials and devices. science. 2002 Sep 27;297(5590):2229-32. https://doi.org/10.1126/science.1072886
[5] Burstein E, Lundqvist S, editors. Tunneling phenomena in solids. New York: Plenum Press; 1969. https://doi.org/10.1007/978-1-4684-1752-4
[6] Bartkowiak M, Mahan GD. Boundary effects in thin-film thermoelectrics. MRS Online Proceedings Library (OPL). 1998 Jan;545:265. https://doi.org/10.1557/proc-545-265
[7] Da Silva LW, Kaviany M. Micro-thermoelectric cooler: interfacial effects on thermal and electrical transport. International Journal of Heat and Mass Transfer. 2004 May 1;47(10-11):2417-35. https://doi.org/10.1016/j.ijheatmasstransfer.2003.11.024
[8] Anatychuk LI, Bulat LP. Semiconductors under extreme temperature conditions. Saint-Petersburg: Nauka Publ.–224 p. 2001.
[9] Babin VP, Gudkin TS, Dashevskii ZM, Dashevskii LD, Dudkin EK. Lordanishvili, EK; Kaidanov, VI; Kolomoets, NV; Narva, OM; Stil'bans, LS. Anisotropic synthetic thermoelements and their maximum capabilities. Sov. Phys. Semicond. 1974;8:478-81.
[10] Snarskii AO. Effective properties of macroscopically inhomogeneous media with restructuring. Ukrainian journal of physics. 2025(70,№ 10):697-703. https://doi.org/10.15407/ujpe70.10.697
[11] Stratton R. Theory of field emission from semiconductors. Physical Review. 1962 Jan 1;125(1):67. https://doi.org/10.1103/physrev.125.67
[12] Hishinuma Y, Geballe TH, Moyzhes BY, Kenny TW. Refrigeration by combined tunneling and thermionic emission in vacuum: Use of nanometer scale design. Applied Physics Letters. 2001 Apr 23;78(17):2572-4. https://doi.org/10.1063/1.1365944
[13] Landau LD, Bell JS, Kearsley MJ, Pitaevskii LP, Lifshitz EM, Sykes JB. Electrodynamics of continuous media. Elsevier; 2013 Oct 22.
[14] Mahan GD. Thermionic refrigeration. Journal of Applied Physics. 1994 Oct;76(7):4362-6. https://doi.org/10.1063/1.357324
[15] Mahan GD. Multilayer thermionic refrigeration. In Eighteenth International Conference on Thermoelectrics. Proceedings, ICT'99 (Cat. No. 99TH8407) 1999 Aug 29 (pp. 584-589). IEEE. https://doi.org/10.1109/ict.1999.843457